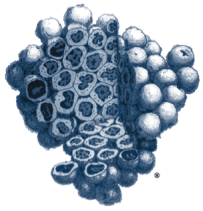

STEM CELLS®

Fibroblast Growth Factor 2 Modulates Transforming Growth Factor ß Signaling in Mouse Embryonic Fibroblasts and Human ESCs (hESCs) to Support hESC Self-Renewal

Boris Greber, Hans Lehrach and James Adjaye

Stem Cells 2007;25;455-464; originally published online Oct 12, 2006;
DOI: 10.1634/stemcells.2006-0476

STEM CELLS®

EMBRYONIC STEM CELLS: CHARACTERIZATION SERIES

Fibroblast Growth Factor 2 Modulates Transforming Growth Factor β Signaling in Mouse Embryonic Fibroblasts and Human ESCs (hESCs) to Support hESC Self-Renewal

BORIS GREBER, HANS LEHRACH, JAMES ADJAYE

Department of Vertebrate Genomics, Max Planck Institute for Molecular Genetics, Berlin, Germany

Key Words. Human ESCs • Self-renewal • Mouse embryonic fibroblasts • Basic fibroblast growth factor

ABSTRACT

Fibroblast growth factor 2 (FGF2) is known to promote self-renewal of human embryonic stem cells (hESCs). In addition, it has been shown that transforming growth factor β (TGFβ) signaling is crucial in that the TGFβ/Activin/Nodal branch of the pathway needs to be activated and the bone morphogenic protein (BMP)/GDF branch repressed to prevent differentiation. This holds particularly true for Serum Replacement-based medium containing BMP-like activity. We have reinvestigated a widely used protocol for conditioning hESC medium with mouse embryonic fibroblasts (MEFs). We show that FGF2 acts on MEFs to release supportive factors and reduce differentiation-inducing activity. FGF2 stimulation experiments with supportive and nonsupportive MEFs followed by genome-wide expression profiling revealed that FGF2 regulates the expression of key members of the TGFβ pathway, with *Inhba*, *Tgfb1*, *Grem1*, and *Bmp4* being the most likely candidates orchestrating the above activities. In addition, restimulation experiments in hESCs combined with global expression analysis revealed downstream targets of FGF2 signaling in these cells. Among these were the same factors previously identified in MEFs, thus suggesting that FGF2, at least in part, promotes self-renewal of hESCs by modulating the expression of TGFβ ligands, which, in turn, act on hESCs in a concerted and autocrine manner. STEM CELLS *2007;25:455–464*

INTRODUCTION

Human embryonic stem cells (hESCs), like mouse ESCs, are pluripotent and self-renewing cells derived from the inner cell mass of blastocysts. hESCs were originally derived in serum-containing medium and on feeder layers of inactivated mouse embryonic fibroblasts (MEFs) that supported hESCs, allowing them to maintain their undifferentiated state [1]. By substituting fetal calf serum with a combination of the proprietary Knockout Serum Replacement (SR) [2] and basic fibroblast growth factor (fibroblast growth factor 2 [FGF2]), Amit et al. [3] demonstrated enhanced cloning efficiencies and reduced the degree of spontaneous differentiation. Subsequently, Xu et al. [4] developed a feeder-free hESC culture system that involves the conditioning of Amit's medium by MEFs and growing hESCs on Matrigel [5], a basement membrane preparation extracted from a murine Engelbreth-Holm-Swarm sarcoma. Hence, MEFs produce soluble factors that are required for the undifferentiated growth of hESCs. Recently, successful attempts have been made to develop chemically defined culture medium [6–8]. All these formulations require the addition of FGF2. In this regard, FGF2 appears to be of similar importance for hESC self-renewal as leukemia inhibitory factor (LIF) is for mouse ESCs [9].

In addition to LIF-mediated activation of STAT3, mouse ESCs require BMP4 signaling to prevent differentiation to the neural lineage [10]. On the contrary, hESCs do not respond to LIF [11, 12], and BMP4 induces differentiation to primitive endoderm or along the trophoblast lineage [13, 14]. Given that Serum Replacement contains BMP-like activity, hESCs may be maintained in unconditioned SR-containing medium under high levels of FGF2 and a BMP antagonist [15, 16]. BMP4 belongs to the transforming growth factor β (TGFβ) superfamily of ligands and stimulates the activation of SMAD 1/5/8 signaling. In contrast, TGFβ, Activin, and Nodal bind to a different set of receptors that activate SMAD 2/3 [17]. Activation of SMAD 2/3 signaling is required for the maintenance of the undifferentiated state [18], and recent reports suggest that supplementation of the culture medium with Activin A may be sufficient to promote self-renewal of hESCs [19, 20]. Also, TGFβ1 and Nodal have been shown to inhibit differentiation [6, 21, 22]. In particular, TGFβ1 has been suggested to prevent hESC differentiation along the primitive endoderm lineage [23].

Using an inhibitor of ALK 4/5/7 to inactivate SMAD 2/3 signaling, Vallier et al. [24] showed that the beneficial effect of FGF2 signaling is dependent on a functional ALK 4/5/7 receptor pathway. In contrast, Xiao et al. [20] presented data suggesting that Activin A induces expression of *FGF2* in hESCs. Hence, there is some controversy as to whether FGF2 signaling or the TGFβ/Activin/Nodal branch of the TGFβ pathway plays the dominant role in sustaining pluripotency of hESCs.

The widely used protocol for feeder-free hESC culture in MEF-conditioned medium [4] involves the supplementation with FGF2 both in the conditioning and the hESC culturing steps. We have reinvestigated the rationale for stimulating both MEFs and hESCs with FGF2, which led us to elucidate the

Correspondence: James Adjaye, Ph.D., Department of Vertebrate Genomics, Max Planck Institute for Molecular Genetics, Ihnestrasse 73, Berlin D-14195, Germany. Telephone: 49-30-8413-1203; Fax: 49-30-8413-1128; e-mail: adjaye@molgen.mpg.de or Boris Greber, Ph.D., Telephone: 49-30-8413-1237; Fax: 49-30-8413-1128; e-mail: greber@molgen.mpg.de Received July 27, 2006; accepted for publication September 30, 2006; first published online in STEM CELLS *EXPRESS* October 12, 2006. 1066-5099/2007/$30.00/0 doi: 10.1634/stemcells.2006-0476

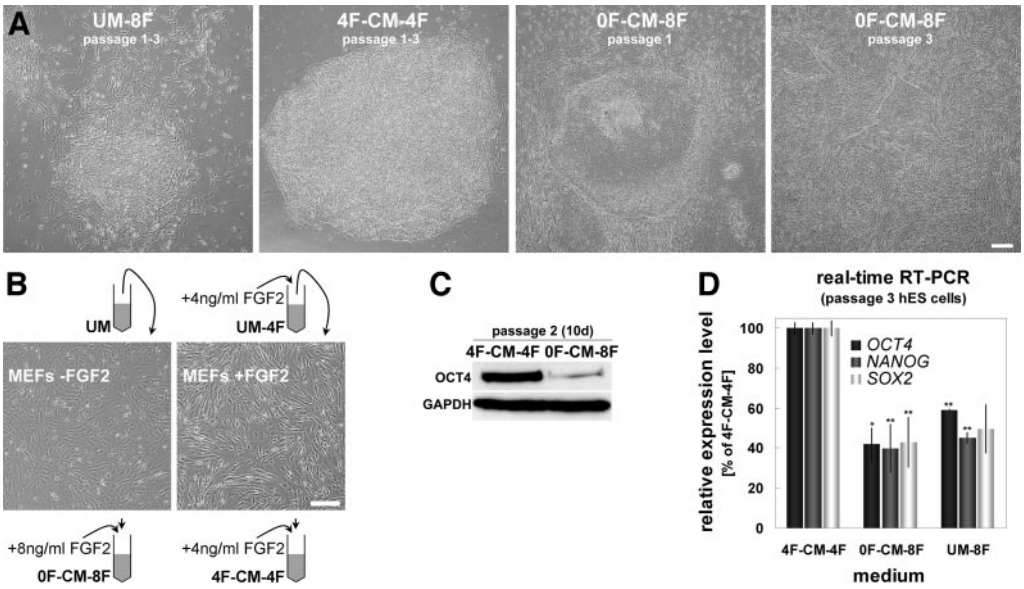

Figure 1. Medium conditioned in the absence of FGF2 fails to sustain human ESC (hESC) self-renewal. **(A):** Representative morphology of H9 hESCs grown in UM-8F, 4F-CM-4F, and 0F-CM-8F. Scale bar = 0.2 mm. **(B):** Schematic for the production of 0F-CM-8F versus 4F-CM-4F and morphology of MEFs without and 1 day after FGF2 treatment (4 ng/ml). The same number of cells was plated in both samples. Scale bar = 0.2 mm. **(C):** Western blot of hESCs grown in the indicated media and probed with OCT4 and GAPDH antibodies. **(D):** Real-time RT-PCR analysis of hESCs grown in the indicated media using primers for pluripotency markers. Bars indicate SE between biological replicates (0F-CM-8F and UM-8F; n = 2–3) or technical variation (4F-CM-4F). Abbreviations: 0F-CM-8F, conditioned medium supplemented with 8 ng/ml FGF2 only after conditioning; 4F-CM-4F, conditioned medium with FGF2 addition before and after the conditioning step; CM, conditioned medium; d, days; FGF2, fibroblast growth factor 2; GAPDH, glyceraldehyde-3-phosphate dehydrogenase; hES, human embryonic stem; MEF, mouse embryonic fibroblast; RT-PCR, reverse transcription-polymerase chain reaction; UM, unconditioned medium; UM-8F, unconditioned medium supplemented with 8 ng/ml FGF2.

immediate downstream targets of FGF2 signaling in both cell types.

Materials and Methods

MEF Cell Culture

MEFs were isolated according to standard procedures [25] from day 12.5 embryos of outbred strains CF1, NMRI, and CD1. Pregnant CF1 females were directly obtained from Harlan/USA (Indianapolis, http://www.harlan.com) (CF-1, code Hsd:NSA). NMRI and CD1 (CD-1) mice were purchased from Harlan/Germany (Borchen, Germany, http://www.harlaneurope.com) and Harlan/France (Gannat, France, http://www.harlaneurope.com), respectively (codes Hsd-Win:NMRI and Hsd:ICR) and bred strainwise for 1–2 generations before MEF isolation. The cells were expanded in high-glucose Dulbecco's modified Eagle's medium (DMEM) containing 10% (vol/vol) fetal calf serum (Biochrom AG, Berlin, http://www.biochrom.de), 2 mM L-glutamine, and penicillin/streptomycin. For production of conditioned media, as well as for FGF2 stimulation experiments, passage 3–5 MEFs were inactivated using mitomycin-C and replated on gelatin-coated dishes at 55,000 cells per square centimeter. The next day, medium was replaced by basic human embryonic stem (hES) medium (unconditioned medium [UM]) at 0.5 ml/cm^2 consisting of Knockout DMEM, 20% (vol/vol) Serum Replacement, 1× nonessential amino acids, 2 mM L-glutamine, penicillin/streptomycin (all from Invitrogen, Carlsbad, CA, http://www.invitrogen.com), and 0.1 mM β-mercaptoethanol. Recombinant human basic fibroblast growth factor (Peprotech, Rocky Hill, NJ, http://www.peprotech.com) was added as appropriate (0 or 4 ng/ml for production of 0F-conditioned medium [CM] and 4F-CM, respectively; 0, 4, 13, and 40 ng/ml for FGF2 stimulation experiments). CM was collected daily for a total of 5 days per batch. Before feeding hESCs, 0F-CM and 4F-CM were supplemented with 8 and 4 ng/ml FGF2, respectively, to yield 0F-CM-8F and 4F-CM-4F (Fig. 1B). RNA from FGF2-treated and untreated MEFs was isolated using Qiagen RNeasy kits (Hilden, Germany, http://www1.qiagen.com) with on-column DNase I digestion 1 day after FGF2 stimulation.

hESC Culture

H1 and H9 hESCs [1] were purchased from WiCell Research Institute (Madison, WI, http://www.wicell.org) at passages 45 and 41, respectively, expanded on feeders, adapted to feeder-free culture in MEF-CM for 2 passages, and then used for subsequent experiments. hESCs were confirmed to stain positive for alkaline phosphatase, OCT4, SSEA-4, TRA-1-60, and TRA-1-81 and negative for SSEA-1 (ES Cell Characterization Kit; Chemicon, Temecula, CA, http://www.chemicon.com). hESCs were replated onto six wells precoated with 1 ml of 1/30 (vol/vol) growth factor-reduced Matrigel (BD Biosciences, San Diego, http://www.bdbiosciences.com), using a combination of mechanical and enzymatic passaging. Briefly, 5-day-old colonies were cut into aggregates of 100–200 cells using a sterile metal needle before the addition of dispase for 5 minutes (1.5 mg/ml). After extensive washing with UM, the complete contents of the wells were dislodged using a sharp plastic scraper, centrifuged to collect clumps of both undifferentiated and differentiated cells, and replated in the appropriate medium at various splitting ratios (1:2–1:4). This was to compensate for reduced plating efficiencies with UM-8F and 0F-CM-8F as compared with 4F-CM-4F. Representative morphology was recorded at a total magnification of ×50 using an Olympus CK2 phase contrast microscope (Tokyo, http://www.olympus-global.com). Protein was extracted in Nonidet P40 and Benzonase-containing buffer. RNA was isolated as indicated above.

Fibroblast-like differentiated cells were derived from H9 hESCs grown in 0F-CM-8F for 3 passages by mechanical removal of remaining undifferentiated colonies. The differentiated cells were further selected by trypsinization and could be expanded in either serum-containing MEF medium (described above), 4F-CM-4F, or—at somewhat lower growth rates—in 0F-CM-8F, but not in unconditioned medium supplemented with or without FGF2 or recombinant insulin-like growth factor 1 (IGF-I) (R&D Systems Inc., Minneapolis, http://www.rndsystems.com). Conditioned medium from human embryonic

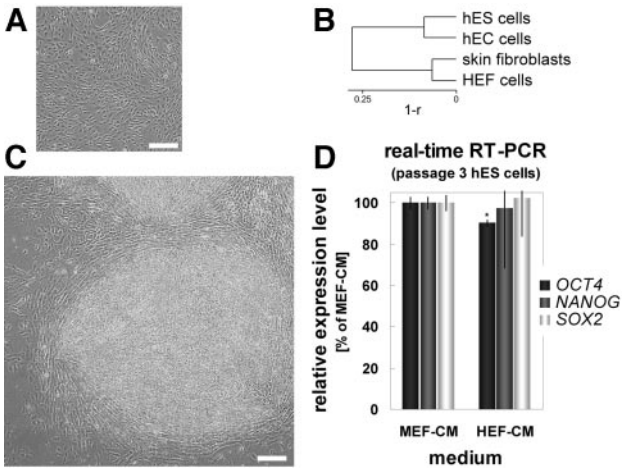

Figure 2. Fibroblast-like differentiated H9 cells support growth of parental human ESCs (hESCs). **(A):** Morphology of H9-derived HEF cells during expansion. Scale bar = 0.2 mm. **(B):** Transcriptome comparison between H9 hESCs, hEC cells (line NCCIT), human skin fibroblasts, and HEF cells, based on microarray data; r = linear correlation coefficient. **(C):** Representative morphology of H9 hESCs grown in medium conditioned by HEF cells. Scale bar = 0.2 mm. **(D):** *OCT4*, *NANOG*, and *SOX2* expression level comparison of H9 cells grown in conventional MEF-CM and medium conditioned by HEF cells. Bars indicate standard errors between independent experiments (HEF-CM; $n = 3$) or technical variation (MEF-CM). Abbreviations: CM, conditioned medium; hEC, human embryonal carcinoma; HEF, human embryonic fibroblast-like; hES, human embryonic stem; MEF, mouse embryonic fibroblast; RT-PCR, reverse transcription-polymerase chain reaction.

fibroblast-like (HEF) cells was prepared as with MEFs. For transcriptome comparisons on gene expression chips (described below), we used H9 hESCs grown in conventional MEF-CM, as well as NCCIT embryonal carcinoma cells [26] (a kind gift of Dr. L. Looijenga) and human foreskin fibroblasts (CRL-2429; American Type Culture Collection, Manassas, VA, http://www.atcc.org) grown in MEF medium.

For assaying SMAD2 phosphorylation, H9 hESCs were maintained undifferentiated in 4F-CM-4F for 3 days before exchange to the following media: (a) 4F-CM; (b) 0F-CM; (c) unconditioned medium supplemented with 20 ng/ml recombinant Activin A, 2 ng/ml TGFβ1 (in line with Fig. 4E), and 250 ng/ml gremlin 1 (all from R&D Systems); (d) 4F-CM plus 10 μM ALK 4/5/7 inhibitor SB431542 (Sigma-Aldrich, St. Louis, http://www.sigmaaldrich.com). All samples were treated in the absence of recombinant FGF2 and with 30 μM SU5402 (Calbiochem, San Diego, http://www.emdbiosciences.com), a potent inhibitor of FGF receptor function [27], to suppress any FGF signaling in this experiment. Protein was extracted after 12 hours of exposure to the four different media.

In FGF2 restimulation experiments, hESCs were grown in 4F-CM-4F for 2 days, starved in UM without FGF2 and with 30 μM of SU5402 for 24 hours, and, after extensive washing, retreated with 40 ng/ml FGF2 in UM for 4 hours. Controls were FGF2-starved but not restimulated. After the FGF2 starvation period, the cells did not show any obvious signs of spontaneous differentiation, as judged by morphological criteria and monitored by OCT4 immunocytochemistry (supplemental online Fig. 1).

Real-Time Reverse Transcriptase-Polymerase Chain Reaction, Western Blotting, Immunocytochemistry, and Enzyme-Linked Immunosorbent Assay

RNA was reverse-transcribed using Moloney murine leukemia virus (USB) and oligo(dT) priming following the manufacturer's instructions. Real-time reverse transcriptase polymerase chain reaction (RT-PCR) was carried out on Applied Biosystems 7900 (Foster City, CA, http://www.appliedbiosystems.com) instrumentation in 20-μl reactions containing 10 μl of SYBR Green PCR mix (ABI), 0.375 μM each primer, and diluted cDNA. All primer pairs used were confirmed to approximately double the amount of product within one cycle and to yield a single product of the predicted size. Primer sequences are provided in supplemental online Table 5. Relative mRNA levels were calculated using the comparative C_T method (ABI instruction manual) and presented either as percentage of housekeeping gene expression or as percentage of biological controls. In all cases, results were essentially independent of the gene used for normalization (*Gapdh* vs. *Actb*). Where appropriate, statistical significance was evaluated using Student's t test (Figs. 1, 2, 4, $*$, $p < .05$; $**$, $p < .01$).

Western blotting was performed on 10–30-μg protein samples separated by SDS-polyacrylamide gel electrophoresis and transferred onto nitrocellulose membranes. Primary antibodies used were Santa Cruz Biotechnology sc-8629 (1/5,000; Santa Cruz, CA, http://www.scbt.com), Ambion 4300 (1/5,000; Austin, TX, http://www.ambion.com), and Cell Signaling Technology 3102 and 3108 (both at 1/1,000; Beverly, MA, http://www.cellsignal.com). Appropriate peroxidase-conjugated secondary antibodies in conjunction with enhanced chemiluminescence detection kits and films (Amersham Biosciences, Piscataway, NJ, http://www.amersham.com) were used for visualization. OCT4 immunostaining was performed using antibodies sc-8629 (1/100; Santa Cruz Biotechnology) and A21468 (1/300; Amersham Biosciences). Enzyme-linked immunosorbent assays (ELISAs) were carried out using products 338-AC, MAB3381, BAM3381, MB100B, and DY998 from R&D Systems, following the manufacturer's recommendations. The linear working range of the Activin A assay was between 0.25 and 32 ng/ml.

Chip Hybridizations and Analysis of Whole-Genome Expression Data

Biotin-labeled cRNA was produced by means of a linear amplification kit (IL1791; Ambion, Austin, TX, http://www.ambion.com) using 300 ng of quality-checked total RNA as input. Chip hybridizations, washing, Cy3-streptavidin (Amersham Biosciences) staining, and scanning were performed on an Illumina BeadStation 500 (San Diego, http://www.illumina.com) platform using reagents and following protocols supplied by the manufacturer. cRNA samples were hybridized on Illumina mouse-6 (CF1 MEFs), mouse-8 (NMRI and CD1 MEFs), and human-8 (for all human samples) BeadChips. The mouse-8 and human-8 chips cover approximately 24,000 RefSeq transcripts, whereas the mouse-6 format contains an additional 23,000 features. Annotation information for the individual chip formats is publicly available from Illumina. The inherent manufacturing principle to randomly distribute large populations of oligonucleotide-coated beads across the available positions enables 30 intensity measurements per feature on average, yielding quantitative results [28]. Pilot experiments (not shown) suggested that biological variation was the major cause for variability of the obtained data, which led us to omit technical replicates. We hybridized the following samples: (a) untreated CF1 MEFs (three biological replicates) and samples stimulated with 4, 13, and 40 ng/ml FGF2, (b) NMRI, and (c) CD1 MEFs (each with 40 ng/ml FGF2 treatment and without); (d) untreated H9 hESCs; NCCIT human embryonal carcinoma (hEC) cells; human skin fibroblasts; HEF cells; and (e) FGF2-starved and restimulated H9 hESCs (two biological replicates each). In addition to information provided in supplemental online Tables 1–4, all processed and raw data are available in a MIAME-compliant format via Gene Expression Omnibus (http://www.ncbi.nlm.nih.gov/geo). Accession numbers are (a) GSE5437, (b) GSE5436, (c) GSE5435, (d) GSE5416, and (e) GSE5415, respectively. All basic expression data analysis was carried out using the manufacturer's software BeadStudio 1.0. Raw data were background-subtracted and normalized using the "rank invariant" algorithm, by which negative intensity values may arise (supplemental online Table 1). Normalized data were then filtered for significant expression on the basis of negative control beads in that induced genes were required to be significantly expressed in a given treated condition, whereas repressed genes needed to be expressed in the control state. Selection for differentially expressed genes was performed on the basis of arbitrary thresholds for fold changes plus statistical significance according to an Illumina custom model [28] ($p < .01$). Differentially expressed genes were

further filtered according to Gene Ontology terms using eGOn (http://www.genetools.no) or mapped to KEGG pathways using DAVID 2006 (http://david.abcc.ncifcrf.gov). For both types of analysis, we used GenBank accession numbers represented by the corresponding chip oligonucleotides as input.

RESULTS

Extrinsic FGF2 Signaling Is Crucial for the Production of Effective MEF-Conditioned Medium

According to Xu et al. [4] conditioned medium is prepared by incubating SR-containing medium [3] including 4 ng/ml FGF2 on high-density cultures of inactivated MEFs (4F-CM). Before feeding hESCs grown on Matrigel-coated plates, another 4 ng/ml FGF2 is added (4F-CM-4F). To investigate the importance of supplementing the medium with FGF2 as early as in the conditioning step, an alternative medium was prepared, termed 0F-CM-8F, in which FGF2 was added to a final concentration of 8 ng/ml only after the conditioning step (Fig. 1B). While preparing the two types of conditioned media, we noticed that FGF2 induced a morphological change in the MEFs, yielding more elongated/stringy cells within 1 day (Fig. 1B). We then compared the ability of 4F-CM-4F and 0F-CM-8F to support the undifferentiated growth of H9 hESCs on Matrigel-coated plates. As a control, we also used unconditioned medium supplemented with 8 ng/ml FGF2 (UM-8F). Within 5 days of culture, morphological differences became apparent. H9 cells grown in 4F-CM-4F were almost exclusively forming round and tightly packed colonies with rather defined boundaries, indicative of undifferentiated growth. In contrast, colonies grown in 0F-CM-8F showed differentiation from the inside of the colonies in more than 50% of cases, as well as a fibroblast-like type of differentiation at the colonies' edges. Cells grown in UM-8F formed rather irregularly shaped and relatively loose colonies with differentiation predominantly at the colonies' boundaries (Fig. 1A). Upon further passaging (5 days per passage), colonies grown in 4F-CM-4F and UM-8F retained their morphology; however, the plating efficiencies in UM-8F were significantly reduced compared with 4F-CM-4F. In contrast, at passage 3, the numbers and average sizes of colonies in 0F-CM-8F were further reduced, and the fibroblast-like differentiated cells occupied almost the entire surface area between the colonies. These, however, now looked tightly packed and had defined boundaries (Fig. 1A). We monitored these morphological differences between cells grown in 4F-CM-4F versus 0F-CM-8F by Western blotting using an antibody against the pluripotency marker OCT4. Indeed, the OCT4 level was strongly reduced in 0F-CM-8F as compared with conventional CM (Fig. 1C). The morphological differences described above were reproducible between independent experiments. We routinely quantified the expression levels of *OCT4* and two additional pluripotency markers (*NANOG* and *SOX2*) using real-time RT-PCR in cells cultured with 4F-CM-4F, 0F-CM-8F, and UM-8F for 3 passages. In line with our morphological observations, the expression levels of all three marker genes were strongly reduced in 0F-CM-8F, to levels similar to those in UM-8F (Fig. 1D). The following conclusions/hypotheses can be drawn from these data:

1. FGF2 stimulates the secretion of one or more supportive factors in MEFs (compare 4F-CM-4F vs. UM-8F and 0F-CM-8F in Fig. 1A, 1B, 1D).
2. 0F-CM-8F contains enhanced levels of differentiation-inducing activity (compare 0F-CM-8F vs. UM-8F and 4F-CM-4F in Fig. 1A, 1D).
3. The fibroblast-like cells appearing with 0F-CM-8F upon continuous passaging support the remaining undifferentiated hESCs (compare morphology with 0F-CM-8F, passage 3 vs. passage 1 in Fig. 1A).

Fibroblast-Like Cells Emerging in 0F-CM-8F Support Remaining Undifferentiated hESCs

To test the hypothesis 3, the remaining undifferentiated colonies from passage 3 0F-CM-8F cultures were mechanically removed, and the fibroblast-like human cells expanded without an apparent change in morphology (Fig. 2A). We profiled the transcriptome of these cells on whole-genome expression chips, along with samples of undifferentiated H9 cells, NCCIT human embryonal carcinoma (hEC) cells, and human skin fibroblasts. A correlation-based clustering analysis showed that the H9 derivative cells were very similar to the control human fibroblast line, whereas the undifferentiated parental hESCs clustered together with the hEC cell line (Fig. 2B). Hence, we termed the H9 derivatives HEF cells, in accordance with published work [29]. Furthermore, we inactivated these cells for the production of conditioned hES medium. CM produced with HEF cells was able to support the parental cells throughout the tested time range (4 passages). The colonies appeared tightly packed and overall undifferentiated, with some spontaneous differentiation at the edges (Fig. 2C). Real-time PCR of *OCT4*, *NANOG*, and *SOX2* expression levels was carried out to show that HEF-based CM was almost equally efficient as MEF-CM in maintaining the undifferentiated state of hESCs (Fig. 2D). Taken together, these data suggest that the fibroblast-like differentiated cells emanating from 0F-CM-8F cultures upon continuous passaging (Fig. 1A) do indeed support the remaining undifferentiated cells, which partially compensated for the otherwise nonsupportive character of the 0F-CM-8F medium.

FGF2 Regulates Key Members of the TGFβ Pathway in MEFs

To address conclusions/hypotheses 1 and 2 above, inactivated MEFs of mouse strain CF1 were treated with various doses (0, 4, 13, and 40 ng/ml) of FGF2 in unconditioned hES medium for 24 hours, and global expression analysis was carried out (supplemental online Table 1). Overall, FGF2 treatment caused differential expression of several thousand genes in MEFs. Those with an at least twofold significant change in expression between the FGF2-treated samples and the 0 ng/ml controls were filtered on the basis of Gene Ontology terms "extracellular space" (GO:0005615) and "receptor-binding" (GO:0005102) [30]. This revealed a number of candidate genes, regulated by extrinsic FGF2 signaling and encoding secreted-and-receptor-binding factors. Seventeen of these were upregulated, and 19 were downregulated (Fig. 3A, 3B; supplemental online Table 2). Among other genes of potential interest in the context of hESC self-renewal (e.g., *Wnt5a*, upregulated; *Igf1*, downregulated), these lists included several genes belonging to the TGFβ pathway, namely *Tgfb1*, *Tgfb2*, *Tgfb3*, *Inhba* (encoding Activin A), and *Bmp4*. However, our filtering criteria excluded soluble factors of this pathway that do not act on membrane receptors of target cells directly, such as antagonists of ligands. We therefore mapped all genes showing at least a twofold significant expression change and encoding secreted factors (GO:0005615) to KEGG pathways [31] using DAVID 2006 [32]. This analysis confirmed that members of the TGFβ pathway were significantly overrepresented among the secreted factors regulated by FGF2 ($p < .01$) and revealed several modulators of TGFβ ligands to be differentially expressed, namely thrombospondin 2 and 3, chordin, and gremlin 1. As was to be expected from a specific response to an exogenous stimulus, the mRNA levels of all differentially expressed genes encoding extracellular members of the TGFβ pathway changed in a dose-dependent manner,

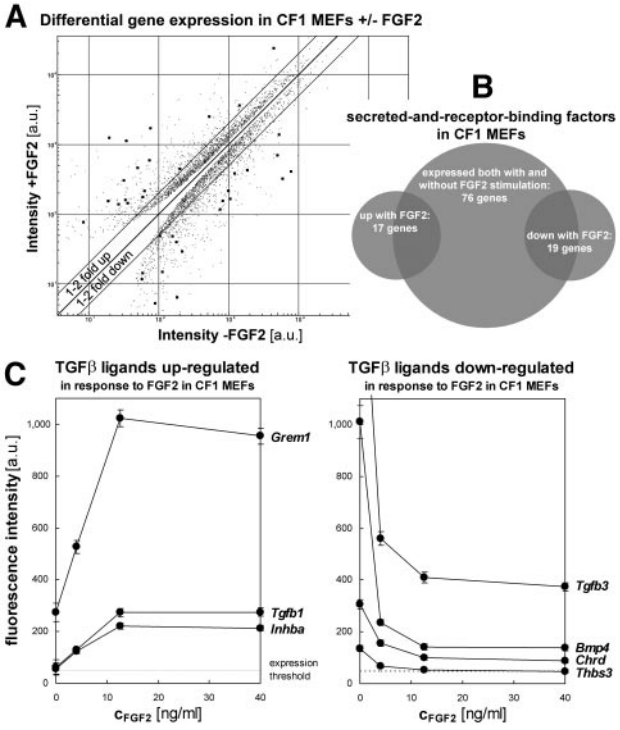

Figure 3. Global gene expression analysis of FGF2-stimulated versus nontreated MEFs. **(A):** Expression data of treated samples plotted against untreated ones ($n = 3$). Small dots represent differentially expressed genes ($p < .01$). Genes encoding secreted-and-receptor-binding proteins are highlighted as enlarged squares. The diagonal lines indicate thresholds for expression level ratios. **(B):** Venn diagram of genes encoding secreted-and-receptor-binding factors in MEFs, based on microarray data shown in **(A)**. Approximately 50% of both the up- and downregulated genes were undetectable in the nontreated and the +FGF2 conditions, respectively. **(C):** Secreted members of the TGFβ pathway are regulated by FGF2 in a dose-dependent manner. Data are arbitrary intensity units extracted from supplemental online Table 1. Standard error bars represent variation between biological replicates (−FGF2 controls) or between Illumina beads (+FGF2 samples). Tgfb2 and Thbs2 were also downregulated but were not included in the chart on the right for reasons of clarity. The expression threshold was set on the basis of negative control beads. Abbreviations: FGF2, fibroblast growth factor 2; MEF, mouse embryonic fibroblast; TGFβ, transforming growth factor β.

showing saturation from approximately 13 ng/ml FGF2 (Fig. 3C). We concluded that the regulation of at least some of these factors by FGF2 may account for the vast difference in the capabilities of 4F-CM-4F and 0F-CM-8F to support the undifferentiated growth of H9 hESCs.

Tgfb1, Inhba, Grem1, and *Bmp4* Are the Genes Expressed in MEFs Most Likely To Influence hESC Self-Renewal

To further confirm the above results, we used a different hESC line, H1, as well as additional batches of MEFs derived from mouse strains other than the widely used CF1, namely NMRI and CD1. To rule out an influence of the H1 passage number, we compared in parallel the performances of CF1-, NMRI-, and CD1-conditioned medium prepared with or without FGF2 supplementation. As before, we obtained early trophoblast-like differentiation in the centers of the colonies [13], as well as differentiation around the colonies after several days in 0F-CM-8F with all three batches of MEFs, whereas H1 cells grown in CF1 and NMRI 4F-CM-4F remained undifferentiated throughout the experiment. Somewhat surprising was the fact that hESCs in CD1 4F-CM-4F differentiated partially, almost to a similar extent as the cells in CF1 and NMRI 4F-CM-4F, but still less than in 0F-CM-8F from the same batch of MEFs (representative morphologies are given in Fig. 4A). To quantify these observations, mRNA expression levels of the core hESC transcription factors OCT4, NANOG, and SOX2 were again recorded using real-time PCR at passage 2 (Fig. 4B). The lack of support by the CD1 4F-CM-4F medium in comparison with the two supportive batches of CF1 and NMRI feeders was confirmed using H9 hESCs in additional experiments (results not shown).

We therefore reasoned that the nonsupportive MEFs could be used to narrow down the list of the previously identified TGFβ candidate genes. To this end, RNA samples from FGF2-stimulated and nontreated MEFs of the second supportive strain and the nonsupportive strains were again hybridized on expression arrays, and differentially expressed genes encoding secreted proteins were identified as before. We then devised a subtractive approach, illustrated in Figure 4C, to select genes encoding secreted factors that are differentially expressed upon FGF2 treatment in both supportive batches of MEFs but not in the nonsupportive ones (supplemental online Table 3). Interestingly, this list included two genes encoding SMAD 2/3 activators, *Tgfb1* and *Inhba*, and one gene coding for a BMP4 antagonist, *Grem1*. The primary candidate for differentiation-inducing activity, *Bmp4*, appeared to be significantly downregulated upon FGF2 treatment in all three MEF batches. However, we noticed that the *Bmp4* expression levels were considerably higher in the nonsupportive MEFs, according to the array data. Therefore, real-time confirmations at several FGF2 concentrations were carried out on *Tgfb1*, *Inhba*, *Grem1*, as well as on *Bmp4* (Fig. 4D). Indeed, using this alternative technique for mRNA level quantification, *Tgfb1*, *Inhba*, and *Grem1* were strongly upregulated in a concentration-dependent manner upon FGF2 treatment, using MEFs of the two supportive strains, whereas the expression levels of these genes did not change or were only slightly induced in the nonsupportive feeder cells. In contrast, *Bmp4* expression levels dropped substantially with increasing doses of FGF2 in all three MEF batches. However, the overall *Bmp4* mRNA levels in the nonsupportive MEFs were substantially higher, especially at moderate concentrations of FGF2 (4 and 13 ng/ml; Fig. 4D).

To test whether these changes in mRNA abundance also become apparent at the protein level, we performed ELISA-based analyses of Activin A and TGFβ1 concentrations in 0F-CM and 4F-CM produced with supportive and nonsupportive MEFs. As shown in Figure 4E, Activin A and TGFβ1 protein levels were approximately 10 times higher in conditioned medium produced from FGF2-stimulated CF1 feeders as compared with 0F-CM of the same cells. In contrast, TGFβ1 and in particular Activin A levels were substantially lower in 4F-CM prepared with nonsupportive CD1 MEFs.

These data suggest that 4F-CM-4F supports hESC self-renewal via activation of SMAD 2/3, in contrast to 0F-CM-8F, which contains only low levels of Activin A and TGFβ1. We sought to demonstrate this by assaying the SMAD2 phosphorylation status in response to the two types of conditioned medium, under FGF2 starving conditions in hESCs. As shown in Figure 4F, SMAD2 phosphorylation was substantially enhanced in 4F-CM as compared with 0F-CM, and this effect could be mimicked by extrinsic supplementation of unconditioned medium with recombinant Activin A, TGFβ1, and gremlin 1. In cells treated with 4F-CM and an inhibitor of TGFβ/Activin/Nodal type I receptors, SMAD2 phosphorylation was abolished, as expected.

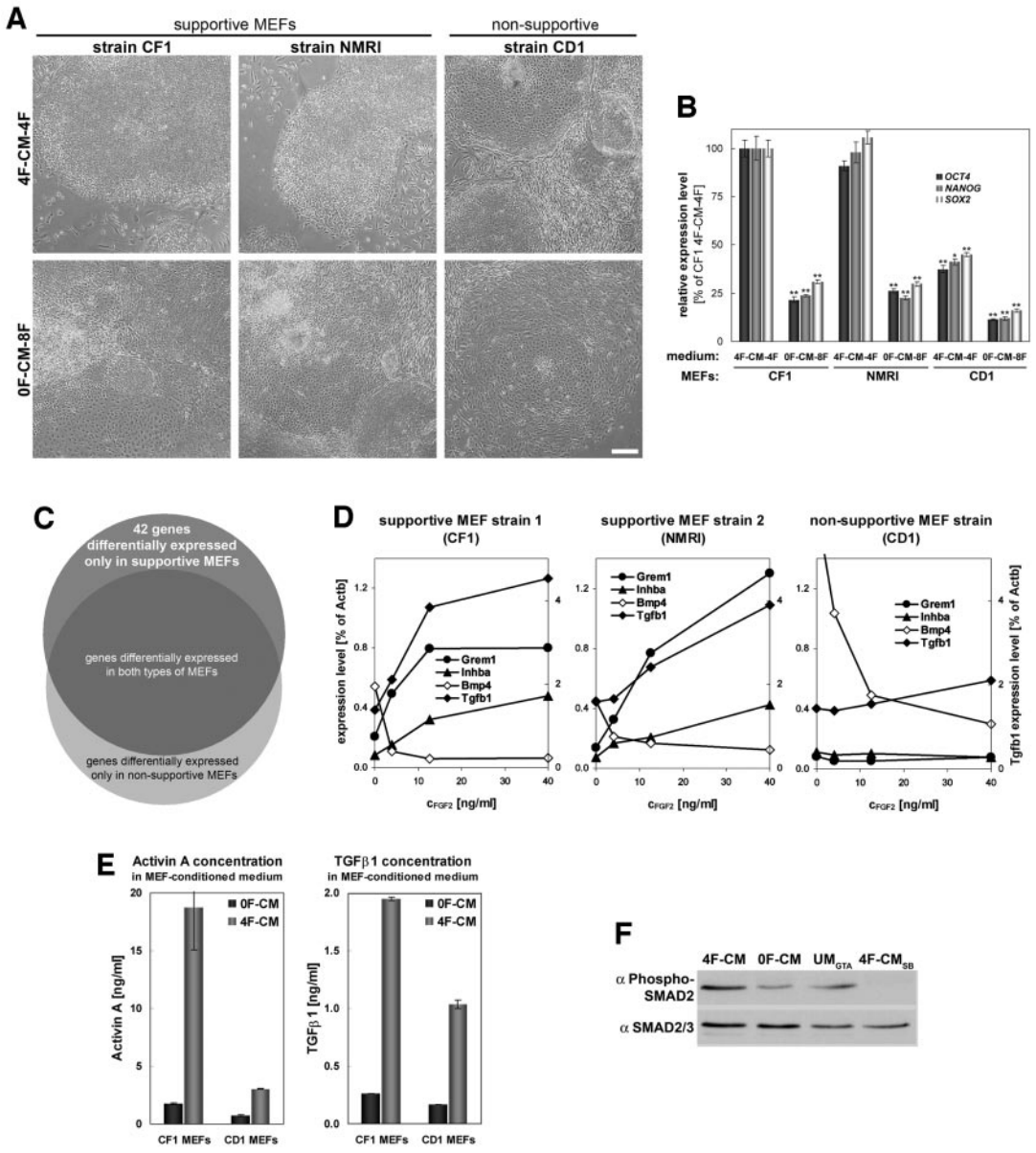

Figure 4. Nonsupportive MEFs may be used to narrow down candidate genes relevant for human ESC (hESC) self-renewal. **(A):** H1 hESCs differentiated rapidly in conditioned medium with FGF2 addition before and after the conditioning step (4F-CM-4F) produced from nonsupportive feeders and in conditioned medium supplemented with 8 ng/ml FGF2 only after conditioning (0F-CM-8F) of all MEF batches tested. Representative pictures were taken from hESC cultures fed with the indicated media for 5 days. Scale bar = 0.2 mm. **(B):** Real-time reverse transcription-polymerase chain reaction (RT-PCR) analyses on samples in **(A)** at the end of passage 2 (10 days) using primers for pluripotency markers. Note the low levels of *OCT4*, *NANOG*, and *SOX2* expression in CD1 4F-CM-4F compared with the two supportive MEF strains. Bars indicate technical standard errors. **(C):** Venn diagram illustrating a subtractive approach to filtering microarray data for genes encoding secreted proteins that are differentially expressed in supportive MEFs (overlap of CF1 and NMRI chip data) in response to FGF2 but not in the nonsupportive feeders. The 42 genes, notably encoding both soluble proteins and constituents of the extracellular matrix, are listed in supplemental online Table 3. **(D):** Real-time RT-PCR analyses of supportive and nonsupportive MEFs treated for 1 day with different doses of FGF2 using primers for upregulated TGFβ pathway members from supplemental online Table 3 and Bmp4. Note that *Bmp4* was downregulated in all cases, but its expression level (as a percentage of Actb) was substantially higher in nonsupportive MEFs compared with those in CF1 and NMRI fibroblasts. The charts are drawn on the same scale to better illustrate this fact. **(E):** Enzyme-linked immunosorbent assay (ELISA)-based measurements of Activin A and TGFβ1 concentrations in 0F-CM and 4F-CM prepared with CF1 and CD1 fibroblasts. In contrast to **(D)** (1 day of FGF2 treatment), CM was collected for 5 days and then pooled. NMRI cells from the same batch used in **(A–D)** were no longer available at the time the ELISAs were conducted. Error bars denote standard deviations between technical replicates ($n = 2$). **(F):** Western blot showing decreased SMAD2 phosphorylation (at Ser465/467) in 0F-CM versus 4F-CM from supportive feeders. Total SMAD 2/3 served as loading control. Note that loading of this sample was somewhat lower than in lanes 1 and 2. Abbreviations: 0F-CM-8F, conditioned medium supplemented with 8 ng/ml FGF2 only after conditioning; 4F-CM-4F, conditioned medium with FGF2 addition before and after the conditioning step; 4F-CM_{SB}, 4F-CM plus ALK 4/5/7 inhibitor SB431542; Bmp, bone morphogenic protein; FGF2, fibroblast growth factor 2; MEF, mouse embryonic fibroblast; TGF, transforming growth factor; UM_{GTA}, unconditioned medium supplemented with recombinant gremlin 1, TGFβ1, and Activin A to mimic 4F-CM.

Downstream Targets of FGF2 Signaling in hESCs

According to Xu et al. [4], FGF2 is repeatedly added to the culture medium after the conditioning step. We confirmed the importance of this step by omitting it (results not shown). These tests encouraged us to investigate the downstream targets of direct FGF2 signaling in hESCs. FGF2 is expressed by hESCs and autocrine FGF2 signaling plays an important role [33]. Therefore, FGF2 restimulation (rather than withdrawal) experiments were carried out, and samples were once again hybridized on expression chips to reveal the immediate downstream effects on gene expression, caused by the restimulation event. The differentially expressed genes are presented in supplemental online Table 4. Overall, there was a bias toward the upregulation of genes (478 up- vs. 114 genes downregulated; ratio, >1.5; $p < .01$). Confirming the design of the restimulation experiments, the upregulated genes included *FOS*, a recently described downstream target of FGF2 signaling in hESCs [34], as well as Sprouty and Spred genes (*SPRY1*, *2*, and *4*; *SPRED1* and *2*) which are known to be induced by FGFs and function as negative feedback inhibitors of ERK/MAPK signaling [34–36]. We further annotated differentially expressed genes with Gene Ontology terms to reveal overrepresented functional categories. Interestingly, there were more than 30 genes involved in cell cycle regulation (GO:0007049; supplemental online Table 4), suggesting that FGF2 is regulating genes associated with hESC proliferation, as well as more than 40 genes encoding transcription factors (GO:0003700; supplemental online Table 4), revealing complex downstream effects of FGF2 signaling in hESCs. Transcription factors upregulated in response to FGF2 stimulation included zinc finger proteins, SRY- and forkhead box TFs (*SOX4*, *-8*, and *-13*; *FOXC2*, *-D1*, and *-L2*), cellular oncogenes (*FOS*, *JUN*, *MYC*, and *ETS2*), and, interestingly, the pluripotency controlling gene *NANOG*.

Moreover, the lists of up- and downregulated FGF2 targets were mapped to known signaling pathways. Using high statistical stringency ($p < .01$), this analysis exclusively revealed members of the TGFβ pathway to be significantly enriched in the set of differentially expressed genes (supplemental online Table 4). Upregulated components included *ACVR1*, *INHBA*, *GREM1*, *SMAD3*, and *THBS1*. *CER1* was upregulated threefold at $p = .03$. Downregulated TGFβ members were *BMP4*, *LEFTB*, and *SMAD6*. This high percentage of genes encoding secreted proteins suggests that FGF2 is regulating these to act on hESCs in an autocrine manner. Therefore, in the context of this study, real-time RT-PCR confirmations of the array results were mainly confined to secreted TGFβ members and known FGF2 target genes. Figure 5A shows that the array-based expression ratios could be confirmed with high confidence in essentially all cases tested.

DISCUSSION

Our reinvestigation of a widely used protocol for feeder-free hESC culture [4] revealed the importance of exogenous FGF2 supplementation in the conditioning step (Fig. 1). Our results suggest that FGF2 stimulates the secretion of beneficial factors in MEFs and suppresses the release of differentiation-inducing activity. These effects were partially compensated for by differentiation of hESCs into a fibroblast-like cell type capable of supporting the remaining undifferentiated cells (Fig. 2). Growth rate experiments in various media suggested that these hESC-derived fibroblasts also require factors released by the MEFs—or, alternatively, fetal calf serum (Materials and Methods). However, differentiation of hESCs into the fibroblast cell type appeared to be favored by medium conditioned in the absence of

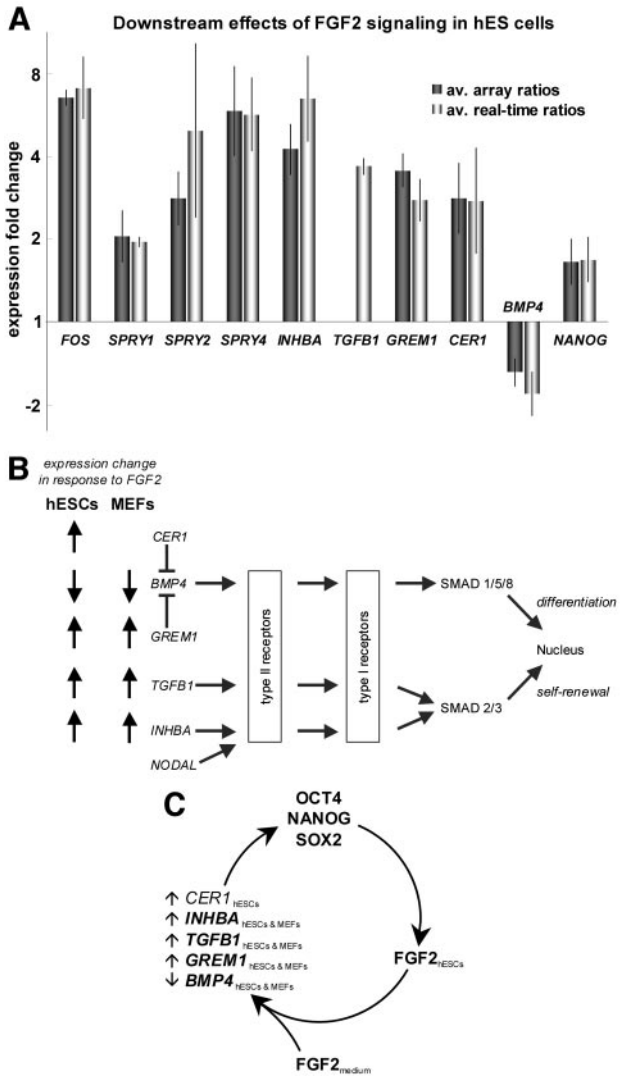

Figure 5. FGF2 regulates key TGFβ members in both MEFs and hESCs, resulting in support of the undifferentiated state. **(A):** Real-time reverse transcription-polymerase chain reaction confirmations of selected genes differentially expressed in response to exogenous FGF2 in hESCs. Array-based expression ratios from supplemental online Table 4 are also shown for comparison. Note the logarithmic scale of the fold changes and the high agreement between the array- and real-time-based measurements. The array oligo for *TGFB1* was found to be falsely designed. Error bars indicate variation between two independent restimulation experiments. **(B):** Simplified scheme of the TGFβ pathway modified from [17] interpreting results from FGF2 stimulation experiments in MEFs and hESCs. Interestingly, upregulated NANOG **(A)** may, in addition, contribute to repression of BMP signaling by directly binding to SMAD1, according to a recent report [54]. Differential expression of the Nodal gene was observed neither in MEFs nor in hESCs. **(C):** Model of regulatory relationships between FGF2, TGFβ pathway, and core hESC transcription factors, integrating results from the present study and published data (supporting evidence given in Discussion). Arrows denote induction or repression of gene transcription. Abbreviations: av., average; BMP, bone morphogenic protein; FGF2, fibroblast growth factor 2; hES, human embryonic stem; hESC, human ESC; MEF, mouse embryonic fibroblast; TGFB1, transforming growth factor β1.

FGF2. Xu et al. [29] described the derivation of a similar if not identical cell type termed HEF1 via the formation of embryoid bodies and subsequent selection in serum-containing medium. Growing hESCs in 0F-CM-8F for several passages followed by

mechanical removal of the few remaining undifferentiated colonies would simplify the derivation and initial scale-up culture of supportive human feeder cells from any parental line, if desired.

FGF2 stimulation of MEFs leads to a morphological change sometimes falsely attributed to the Serum Replacement contained in basic hESC medium (personal communication) and induced overt differential gene expression (Fig. 3A). Regarding the feeder-free growth of hESCs on Matrigel, only genes encoding soluble secreted proteins appeared to be of relevance in this study. We therefore made use of Gene Ontology annotation to filter the large set of genes differentially expressed in response to FGF2. In a stepwise subtractive approach using supportive and nonsupportive batches of MEFs, the list of candidate genes conferring beneficial or detrimental activities in the context of hESC self-renewal was narrowed down essentially to *Tgfb1*, *Inhba*, *Grem1* (all upregulated by FGF2), and *Bmp4* (downregulated), respectively. The effects of the encoded factors on hESC self-renewal are well documented: TGFβ1 and Activin A prevent differentiation via activation of SMAD 2/3 [17, 18, 22, 24], whereas BMP4 initiates differentiation to trophoblast or primitive endoderm via SMAD 1/5/8 signaling [13, 14]. Gremlin is a BMP antagonist that can substitute for MEFs at high doses of FGF2, neutralizing BMP-like activity in SR-containing hESC medium [15]. Hence, FGF2 appears to switch MEFs to an overall hESC-supportive mode through the concerted dysregulation of these factors (Figs. 4D–4F, 5B). This will also apply for feeder-dependent hESC culture in SR-containing medium [3]. Interestingly, Activin A and TGFβ1 protein levels in conditioned medium prepared with supportive feeders matched the physiological range in that they exceeded empirically determined thresholds to prevent hESC differentiation in the case of 4F-CM but not in 0F-CM (Fig. 4E) [6, 20, 23].

There may be additional factors released by MEFs that have an impact on hESC self-renewal. For instance, *Igf1* as a candidate for promoting proliferation of differentiated fibroblast-like cells was strongly downregulated in response to FGF2 (supplemental online Table 2), whereas *Wnt5a* was upregulated exclusively in supportive feeders (supplemental online Table 3). However, preliminary experiments in which we tested recombinant forms of the encoded proteins (0–100 ng/ml) for effects on hESC proliferation and/or differentiation did not reveal evident results (not shown). Pyle et al. [37] recently reported that MEFs express neurotrophins NT3, NT4, and BDNF, which together accounted for most of the antiapoptotic activity of CM when plating hESCs as single cells at low density. We routinely replated hESCs as aggregates of 100–200 cells and monitored differentiation rather than cell survival. Hence, the genes revealed in this study differ from those in the work of Pyle et al. [37]. Somewhat surprisingly, neurotrophins were below detectable levels in our array experiments and consequently are not listed in supplemental online Table 2, which may be explained by the fact that RT-PCR is a more sensitive method for mRNA detection [37].

To test whether FGF2 also regulates key members of the TGFβ pathway in hESCs and to reveal overall downstream targets of FGF2 signaling, restimulation experiments were performed followed by whole-genome expression analysis. The upregulation of known FGF2 target genes and the high degree of consistency with real-time RT-PCR validations suggests that the data set is of high quality (Fig. 5A). To our knowledge, such data has not yet been published and will therefore present a useful basis for further investigation in the field. The gene set presented in supplemental online Table 4 includes large numbers of transcription factors, genes with unknown functions, and additional genes of potential interest such as *GJA7* and *GJB2* (both upregulated) encoding gap junction proteins. This is noteworthy because functional gap junctions have been shown to be present in undifferentiated hESCs [38–40]. Furthermore, FGF2 treatment caused differential expression of large numbers of cell cycle-related genes and induced cellular oncogenes (*FOS*, *JUN*, *MYC*, and *ETS2*), in line with its ability to stimulate cellular proliferation. In addition, 10 members of the TGFβ pathway were also differentially expressed within 4 hours of FGF2 restimulation (supplemental online Table 4). Although this does not rule out additional signaling pathways being operative in the undifferentiated state, it strongly suggests that FGF2 is an upstream regulator of TGFβ signaling in hESCs. The high proportion of genes encoding secreted TGFβ members raised the interesting hypothesis that FGF2 modulates the levels of these factors, enabling them to act on hESCs in an autocrine way. Strikingly, these were essentially the same genes as those identified in supportive MEFs, namely *INHBA*, *TGFB1*, and *GREM1* being upregulated and *BMP4* being downregulated. In addition, *CER1*, the gene encoding Cerberus, a known Nodal and BMP antagonist highly enriched in hESCs [41, 42], was confirmed to be also upregulated by FGF2 (Fig. 5A). These data are in line with the findings that TGFβ/Activin/Nodal signaling is characteristic and necessary for maintaining the undifferentiated state [18, 24, 43] and that, in contrast, activation of the BMP/GDF branch leads to the loss of pluripotency [13, 14, 18] (Fig. 5B).

Notably, there is some indication of these secondary effects, in that *ID1*, a known downstream target of BMP signaling [44], was repressed approximately threefold after 4 hours of FGF2 restimulation. Likewise, *CDKN2B*, which is induced by Activin A signaling [45], was upregulated approximately twofold (supplemental online Table 4). Therefore, we cannot rule out the possibility that there are additional instances of differential gene expression in the data set mediated by an activity shift from the BMP/GDF toward the TGFβ/Activin/Nodal branch of the TGFβ pathway, downstream of FGF2 signaling. Another example of SMAD 2/3 activation might be the upregulation of *NANOG* (Fig. 5A) [46, 47], as Activin A has been demonstrated to maintain high expression levels of this gene and *OCT4* [18–20, 24]. Furthermore, Boyer et al. and other groups [48 and references therein] have shown that OCT4, NANOG, and SOX2 form the core of transcriptional regulation in hESCs, characterized by reciprocal and autoregulation, as well as promoter occupancy of hundreds of target genes. Interestingly, the genes co-occupied by all three transcription factors included *FGF2* and two genes encoding FGF receptors (*FGFR1* and *FGFR2*). These target genes are expressed in undifferentiated hESCs, indicating positive regulation; moreover, loss of pluripotency correlates with downregulation of FGF2 and its receptors [49–51]. Finally, autocrine FGF2 signaling has been shown to be operative in hESCs, as one may require from any genuine *self*-renewal factor [33]. Taken together, these data suggest a regulatory circuit essential for maintaining self-renewal in hESCs. This is characterized by exogenous and autocrine FGF2 signaling being upstream of key TGFβ ligands that, in a concerted manner, sustain OCT4, NANOG, and SOX2 expression, whereas these, in turn, activate endogenous expression of FGF2 (Fig. 5C). This concept would also be in line with the finding that the beneficial effect of FGF2 signaling is dependent on ALK 4/5/7 receptor function [24].

In SR-based medium containing BMP-like activity, either a very high dose of exogenous FGF2 [52, 53] or a combination of either high FGF2 plus BMP4 antagonist [15, 16] or FGF2 plus MEFs [3, 4] is required to prevent differentiation. It has recently been reported that Activin A supplementation is sufficient for sustaining pluripotency of hESCs in SR-containing medium at moderate concentrations [20]. This probably presents a more direct means of activating SMAD 2/3, thus overriding BMP

activity in the medium. However, the data presented in that study [20] suggesting that Activin A directly upregulates FGF2 expression in hESCs are not stringently conclusive. The stimulation experiments were carried out over a time range of 6 days, which leaves open the possibility of indirect FGF2 upregulation via the core transcription factors OCT4, NANOG, and SOX2 [48], in line with Figure 5C. Moreover, Yao et al. [8] recently reported that FGF2 was sufficient to sustain pluripotency of hESCs in a chemically defined medium, whereas Activin A alone induced differentiation to definitive endoderm under these conditions. This may suggest that the levels of TGFβ ligands acting on hESCs need to be more balanced/regulated for sustaining the undifferentiated state. In support of this idea, Pera et al. [14] found that even low levels of BMP signaling may be required to prevent differentiation to neurectoderm. In conclusion, FGF2 appears to be the most upstream self-renewal factor in human embryonic stem cells.

ACKNOWLEDGMENTS

We are grateful to Drs. Tom Burdon, Wei Cui, and Judy Fletcher for sharing their knowledge of hESC culture. This work was supported by Deutsche Forschungsgemeinschaft Grant DFG-AD 184/4-1.

DISCLOSURES

The authors indicate no potential conflicts of interest.

REFERENCES

1 Thomson JA, Itskovitz-Eldor J, Shapiro SS et al. Embryonic stem cell lines derived from human blastocysts. Science 1998;282:1145–1147.
2 Price PJ, Goldsborough MD, Tilkins ML, inventors. Invitrogen, assignee. Embryonic stem cell serum replacement. International patent WO9830679. July 16, 1998.
3 Amit M, Carpenter MK, Inokuma MS et al. Clonally derived human embryonic stem cell lines maintain pluripotency and proliferative potential for prolonged periods of culture. Dev Biol 2000;227:271–278.
4 Xu C, Inokuma MS, Denham J et al. Feeder-free growth of undifferentiated human embryonic stem cells. Nat Biotechnol 2001;19:971–974.
5 Kleinman HK, McGarvey ML, Hassell JR et al. Basement membrane complexes with biological activity. Biochemistry 1986;25:312–318.
6 Ludwig TE, Levenstein ME, Jones JM et al. Derivation of human embryonic stem cells in defined conditions. Nat Biotechnol 2006;24:185–187.
7 Lu J, Hou R, Booth CJ et al. Defined culture conditions of human embryonic stem cells. Proc Natl Acad Sci U S A 2006;103:5688–5693.
8 Yao S, Chen S, Clark J et al. Long-term self-renewal and directed differentiation of human embryonic stem cells in chemically defined conditions. Proc Natl Acad Sci U S A 2006;103:6907–6912.
9 Chambers I, Smith A. Self-renewal of teratocarcinoma and embryonic stem cells. Oncogene 2004;23:7150–7160.
10 Ying QL, Nichols J, Chambers I et al. BMP induction of Id proteins suppresses differentiation and sustains embryonic stem cell self-renewal in collaboration with STAT3. Cell 2003;115:281–292.
11 Daheron L, Opitz SL, Zaehres H et al. LIF/STAT3 signaling fails to maintain self-renewal of human embryonic stem cells. STEM CELLS 2004;22:770–778.
12 Humphrey RK, Beattie GM, Lopez AD et al. Maintenance of pluripotency in human embryonic stem cells is STAT3 independent. STEM CELLS 2004;22:522–530.
13 Xu RH, Chen X, Li DS et al. BMP4 initiates human embryonic stem cell differentiation to trophoblast. Nat Biotechnol 2002;20:1261–1264.
14 Pera MF, Andrade J, Houssami S et al. Regulation of human embryonic stem cell differentiation by BMP-2 and its antagonist noggin. J Cell Sci 2004;117:1269–1280.
15 Xu RH, Peck RM, Li DS et al. Basic FGF and suppression of BMP signaling sustain undifferentiated proliferation of human ES cells. Nat Methods 2005;2:185–190.
16 Wang G, Zhang H, Zhao Y et al. Noggin and bFGF cooperate to maintain the pluripotency of human embryonic stem cells in the absence of feeder layers. Biochem Biophys Res Commun 2005;330:934–942.
17 Valdimarsdottir G, Mummery C. Functions of the TGFbeta superfamily in human embryonic stem cells [Review]. APMIS 2005;113:773–789.
18 James D, Levine AJ, Besser D et al. TGFbeta/activin/nodal signaling is necessary for the maintenance of pluripotency in human embryonic stem cells. Development 2005;132:1273–1282.
19 Beattie GM, Lopez AD, Bucay N et al. Activin A maintains pluripotency of human embryonic stem cells in the absence of feeder layers. STEM CELLS 2005;23:489–495.
20 Xiao L, Yuan X, Sharkis SJ. Activin a maintains self-renewal and regulates fibroblast growth factor, wnt, and bone morphogenic protein pathways in human embryonic stem cells. STEM CELLS 2006;24:1476–1486.
21 Vallier L, Reynolds D, Pedersen RA. Nodal inhibits differentiation of human embryonic stem cells along the neuroectodermal default pathway. Dev Biol 2004;275:403–421.
22 Amit M, Shariki C, Margulets V et al. Feeder layer- and serum-free culture of human embryonic stem cells. Biol Reprod 2004;70:837–845.
23 Poon E, Clermont F, Firpo MT et al. TGFbeta inhibition of yolk-sac-like differentiation of human embryonic stem-cell-derived embryoid bodies illustrates differences between early mouse and human development. J Cell Sci 2006;119:759–768.
24 Vallier L, Alexander M, Pedersen RA. Activin/Nodal and FGF pathways cooperate to maintain pluripotency of human embryonic stem cells. J Cell Sci 2005;118:4495–4509.
25 Nagy A, Gertsenstein M, Vintersten K et al. Manipulating the Mouse Embryo: A Laboratory Manual. 3rd ed. Cold Spring Harbor, NY: Cold Spring Harbor Laboratory Press, 2003:371–373.
26 Teshima S, Shimosato Y, Hirohashi S et al. Four new human germ cell tumor cell lines. Lab Invest 1988;59:328–336.
27 Mohammadi M, McMahon G, Sun L et al. Structures of the tyrosine kinase domain of fibroblast growth factor receptor in complex with inhibitors. Science 1997;276:955–960.
28 Kuhn K, Baker SC, Chudin E et al. A novel, high-performance random array platform for quantitative gene expression profiling. Genome Res 2004;14:2347–2356.
29 Xu C, Jiang J, Sottile V et al. Immortalized fibroblast-like cells derived from human embryonic stem cells support undifferentiated cell growth. STEM CELLS 2004;22:972–980.
30 Ashburner M, Ball CA, Blake JA et al. Gene ontology: Tool for the unification of biology. The Gene Ontology Consortium. Nat Genet 2000;25:25–29.
31 Kanehisa M. A database for post-genome analysis. Trends Genet 1997;13:375–376.
32 Dennis G Jr, Sherman BT, Hosack DA et al. DAVID: Database for Annotation, Visualization, and Integrated Discovery. Genome Biol 2003;4:P3.
33 Dvorak P, Dvorakova D, Koskova S et al. Expression and potential role of fibroblast growth factor 2 and its receptors in human embryonic stem cells. STEM CELLS 2005;23:1200–1211.
34 Kang HB, Kim JS, Kwon HJ et al. Basic fibroblast growth factor activates ERK and induces c-fos in human embryonic stem cell line MizhES1. STEM CELLS Dev 2005;14:395–401.
35 Wakioka T, Sasaki A, Kato R et al. Spred is a Sprouty-related suppressor of Ras signalling. Nature 2001;412:647–651.
36 Kim HJ, Bar-Sagi D. Modulation of signalling by Sprouty: A developing story. Nat Rev Mol Cell Biol 2004;5:441–450.
37 Pyle AD, Lock LF, Donovan PJ. Neurotrophins mediate human embryonic stem cell survival. Nat Biotechnol 2006;24:344–350.
38 Carpenter MK, Rosler ES, Fisk GJ et al. Properties of four human embryonic stem cell lines maintained in a feeder-free culture system. Dev Dyn 2004;229:243–258.
39 Wong RC, Pebay A, Nguyen LT et al. Presence of functional gap junctions in human embryonic stem cells. STEM CELLS 2004;22:883–889.
40 Huettner JE, Lu A, Qu Y et al. Gap junctions and connexon hemichannels in human embryonic stem cells. STEM CELLS 2006;24:1654–1667
41 Belo JA, Bachiller D, Agius E et al. Cerberus-like is a secreted BMP and nodal antagonist not essential for mouse development. Genesis 2000;26:265–270.
42 Bhattacharya B, Miura T, Brandenberger R et al. Gene expression in human embryonic stem cell lines: Unique molecular signature. Blood 2004;103:2956–2964.
43 Besser D. Expression of nodal, lefty-a, and lefty-B in undifferentiated human embryonic stem cells requires activation of Smad2/3. J Biol Chem 2004;279:45076–45084.
44 Korchynskyi O, ten Dijke P. Identification and functional characterization of distinct critically important bone morphogenetic protein-specific response elements in the Id1 promoter. J Biol Chem 2002;277:4883–4891.

45 Ho J, de Guise C, Kim C et al. Activin induces hepatocyte cell growth arrest through induction of the cyclin-dependent kinase inhibitor p15INK4B and Sp1. Cell Signal 2004;16:693–701.
46 Chambers I, Colby D, Robertson M et al. Functional expression cloning of Nanog, a pluripotency sustaining factor in embryonic stem cells. Cell 2003;113:643–655.
47 Mitsui K, Tokuzawa Y, Itoh H et al. The homeoprotein Nanog is required for maintenance of pluripotency in mouse epiblast and ES cells. Cell 2003;113:631–642.
48 Boyer LA, Lee TI, Cole MF et al. Core transcriptional regulatory circuitry in human embryonic stem cells. Cell 2005;122: 947–956.
49 Brandenberger R, Wei H, Zhang S et al. Transcriptome characterization elucidates signaling networks that control human ES cell growth and differentiation. Nat Biotechnol 2004;22:707–716.
50 Sato N, Sanjuan IM, Heke M et al. Molecular signature of human embryonic stem cells and its comparison with the mouse. Dev Biol 2003;260:404–413.
51 Babaie Y, Herwig R, Greber B et al. Analysis of Oct4-dependent transcriptional networks regulating self-renewal and pluripotency in human embryonic stem cells. STEM CELLS 2007;25:500–510.
52 Wang L, Li L, Menendez P et al. Human embryonic stem cells maintained in the absence of mouse embryonic fibroblasts or conditioned media are capable of hematopoietic development. Blood 2005; 105:4598–4603.
53 Levenstein ME, Ludwig TE, Xu RH et al. Basic fibroblast growth factor support of human embryonic stem cell self-renewal. STEM CELLS 2006;24:568–574.
54 Suzuki A, Raya A, Kawakami Y et al. Nanog binds to Smad1 and blocks bone morphogenetic protein-induced differentiation of embryonic stem cells. Proc Natl Acad Sci U S A 2006.


See www.StemCells.com for supplemental material available online.

Fibroblast Growth Factor 2 Modulates Transforming Growth Factor ß Signaling in Mouse Embryonic Fibroblasts and Human ESCs (hESCs) to Support hESC Self-Renewal

Boris Greber, Hans Lehrach and James Adjaye

Stem Cells 2007;25;455-464; originally published online Oct 12, 2006;
DOI: 10.1634/stemcells.2006-0476